Single-Phase PWM Rectifier Using a Model-Based Approach in High-Speed Railway Electrical Traction System

[1]VINAY KUMAR KUCHANA, [2]SK VALI, [3] Ravikumar K

[1,2,3]Assistant Professor
Department of Electrical & Electronics Engineering,
Bhoj Reddy Engg College for Women, Telangana, India.

***Abstract*—The converter with a single-phase rectifier, a dc-link circuit and a three-phase inverter is widely applied in high-speed railway electrical traction drive system. The fault frequency of single-phase rectifier is higher than that of three-phase inverter. Thus, this paper presents a new and fast model-based approach for open-switch fault diagnosis of the single-phase pulse width modulation rectifier, based on the mixed logical dynamic model and residual generation. It requires no additional hardware but only some measurements and command signals which are available in control system. This diagnosis method is quite suitable for electrical traction application due to the fast diagnosis time, simple structure and high reliability. Experimental results confirm the effectiveness and accuracy of the proposed algorithm. It is shown that such diagnosis method can locate the faulty switch in a few milliseconds which is important to avoid catastrophic consequences.**

***Index Terms*—Fault diagnosis, mixed logical dynamic (MLD) model, open-switch fault, single-phase PWM rectifier.**

I. INTRODUCTION

FOR high-speed railway electrical drive systems, ac drive systems has been widely applied in the industry due to the advantages in performance, reliability, lighter quality and lower loss, as compared to dc systems [1]–[3]. Fig. 1 shows a back to-back converter used in electrical railway traction systems, which is made up of a single-phase ac–dc converter on the grid side and three-phase dc–ac inverter on the motor-side.

Usually such electric drive systems are susceptible to electrical faults under complex operating conditions such as static electricity, corrosion, humidity, and temperature. It was reported in [4] that around 38% of the faults in variable-speed ac drives are due to Failures of power semiconductor devices. For high-speed railway electrical traction systems at high power and high voltage, the drive system has very strict reliability and safety requirements. An unexpected failure in the power devices may trigger the protection of the traction control units (TCU) to force shutdown to avoid catastrophic subsequent failures which may jeopardize the safety of passengers. This also results in heavy economic penalties due to unit unavailability and maintenance costs. As a result, condition monitoring and fault diagnostics are highly desirable and necessary for power traction converters

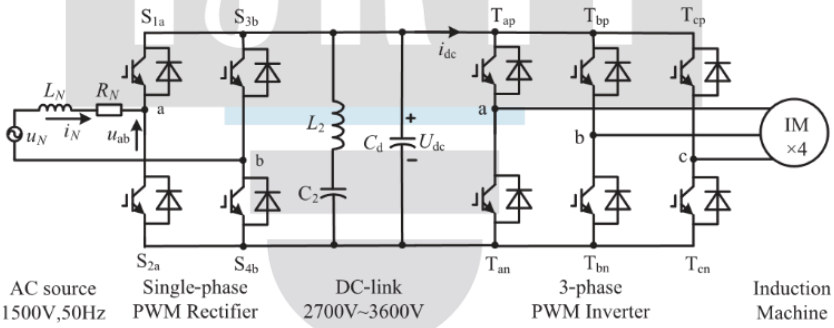

Fig. 1.The strucutre of the AC-DC-AC electrical railway traction system.

The *in situ* diagnostic and prognostic technology to monitor the health condition of insulated gate bipolar transistors(IGBTs) used in electric vehicle with a focus on the IGBTs' solder layer fatigue and wire-bond-related failure have been presented in [5] and [6]. Diagnostic approaches for faults in the IGBT switches in three-phase PWM inverters have been reported in [7]. Only open-circuit faults or misfiring faults in the PWM inverter are mentioned in this reference, since a short-circuit fault in IGBT can be protected by fast-acting fuses resulting in an open circuit.

All methods of fault diagnosis can be classified as either model-based, signal-based, or knowledge-based. Model-based approaches such as the parity space method or observer-based methods have been widely used to detect the faults of power drive systems [8]–[10]. A fault detection method based on a sliding mode observer for open-switch faults in modular multilevel converters

has been reported in [11]. In addition, nonlinear observers were applied to detect and isolate the open switch faults in induction motor drives [12]. A current residual vector-based open-circuit fault diagnostic method for inverters in permanent magnet synchronous motor (PMSM) drive systems has been presented in [13]. An open-switch fault detection and identification method based on model reference adaptive system was proposed for PWM inverters employing a PMSM [14]. Although these methods are load independent, and do not require additional sensors, their performance depends highly on the accuracy of the model and parameter estimation.

Signal-based approaches to detect open-switch fault are classified as current-based [15], [16] and voltage-based [17], [18]. Current-based methods have been widely applied to the fault detection for converters since there is no dependence on system parameters and no need additional hardware. However, the drawbacks of these approaches are slow detection and significant load sensitivity. On the other hand, voltage-based methods give fast fault detection, but require voltage sensors, which may increase the complexity and cost of the drive system substantially. In order to overcome these drawbacks, a new voltage based method without additional sensors for open-switch fault detection of PWM converters was proposed in [19], using information from the reference voltages.

Knowledge-based methods, such as wavelet fuzzy networks [20], wavelet neural networks [21], [22] and expert systems

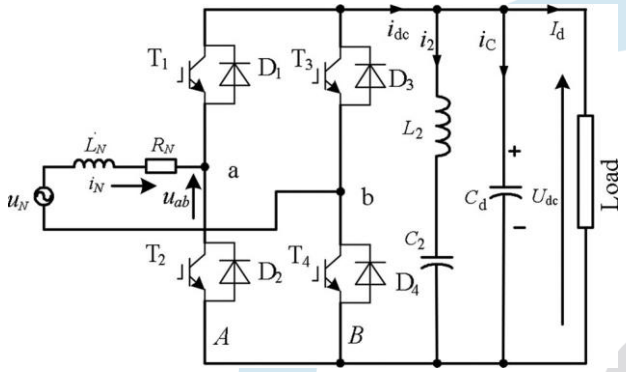

Fig. 2. Topology of the single-phase PWM rectifier circuit.

TABLEI
TRUTH TABLEOF S_A AND S_B

i_N	s_1	s_2	s_3	s_4	S_A	S_B	i_N	s_1	s_2	s_3	s_4	S_A	S_B
$i_N > 0$	0	0	0	0	1	0	$i_N < 0$	0	0	0	0	0	1
	0	0	0	1	1	0		0	0	0	1	0	0
	0	0	1	0	1	1		0	0	1	0	0	1
	0	1	0	0	0	0		0	1	0	0	0	1
	0	1	0	1	0	0		0	1	0	1	0	0
	0	1	1	0	0	1		0	1	1	0	0	1
	1	0	0	0	1	0		1	0	0	0	1	1
	1	0	0	1	1	0		1	0	0	1	1	0
	1	0	1	0	1	1		1	0	1	0	1	1

[23] are also drawing significant attention in fault diagnostics for power devices. An artificial intelligence-based approach to detect the faults of cascaded H-bridge converter was presented in[21].In addition, a multi class neural network method was proposed in [24] to detect the single open-switch fault in a closedloop scenario of the three-phase inverter. These knowledge based algorithms do not require an accurate system model, but do require a long training period and excessive computational effort to achieve good performance.

Surveys regarding open-switch fault diagnosis methods for the three-phase PWM inverters have been reported in [25] and [26].However, open-switch fault diagnosis method related to the single-phase PWM rectifier is rarely found. In[27],the operation of the single-phase PWM rectifier under faulty conditions has been investigated and an open-switch fault detection method which analyzes the average value of the catenary current has been presented. However, this method can only detect the faulty IGBT switch pairs T_1T_4 or T_2T_3 in the single-phase PWM rectifier circuit as shown in Fig. 2, whereas the faulty switch cannot be located. A continuous condition monitor method for single-phase H-bridge converters by adding an additional current sensor was suggested in [28]. A fault detection and fault tolerant control method based on a state observer for the sensors in a single-phase rectifier has been proposed in [29].

The fault frequency of power modules in the grid-side rectifier is higher than that of the motor-side inverter, due to the more complicated operating condition and higher harmonic components [30], [31]. Taking all of these considerations into account, this paper proposes a new open-switch fault diagnosis approach based on the MLD-based model approach for the open-switch fault diagnosis of the single-phase PWM rectifier in high-speed railway electrical drive applications. It will be shown that owing to the constant frequency control strategy and smaller power fluctuations, the model-based method is quite suitable for single-phase PWM rectifiers. It will be shown that this proposed method cannot only detect a faulty rectifier, but can also locate the faulty switch without any additional hardware. Only the values of the catenary current, the dc-link voltage and the command signals from the TCU are needed to create the MLD model.

II. OPEN-CIRCUIT FAULT OF RECTIFIER

The rectifier is used to control the active and reactive power flowing through the grid to ensure unity power factor operation, and also to regulate the dc-link voltage. As shown in Fig. 2, u_N and i_N are the grid voltage and the catenary current, respectively. L_N and R_N are the traction winding leakage inductance and resistance, respectively. u_{ab} is the input voltage of the rectifier, L_2 and C_2 are the series resonant circuit inductance and capacitance. C_d is the dc-link capacitance. The switching functions are defined as

$$S_A = \begin{cases} 1 T_1 \text{ or } D_1 \text{ on} \\ 0 T_2 \text{ or } D_2 \text{ on} \end{cases} \qquad S_B = \begin{cases} 1 T_3 \text{ or } D_3 \text{ on} \\ 0 T_4 \text{ or } D_4 \text{ on} \end{cases} \qquad (1)$$

The relationship between S_A,S_B , and s_1-s_4 are given in Table I, where s_1, s_2, s_3, and s_4 are the command signals of IGBTs in the rectifier, T_1-T_4, respectively. Since the upper and the lower switches of the leg cannot be turned on at the same time, s_1 and s_2, s_3 and s_4 cannot be high simultaneously. At the same time, when both s_1 and s_2 are off, there is a dead-time period of PWM or an open-circuit fault in switch T_1 or T_2.In the real traction drive system, both IGBTs and diodes could experience open-circuit fault. Different kinds of open-circuit faults could have different fault characteristics and result in different fault effects.

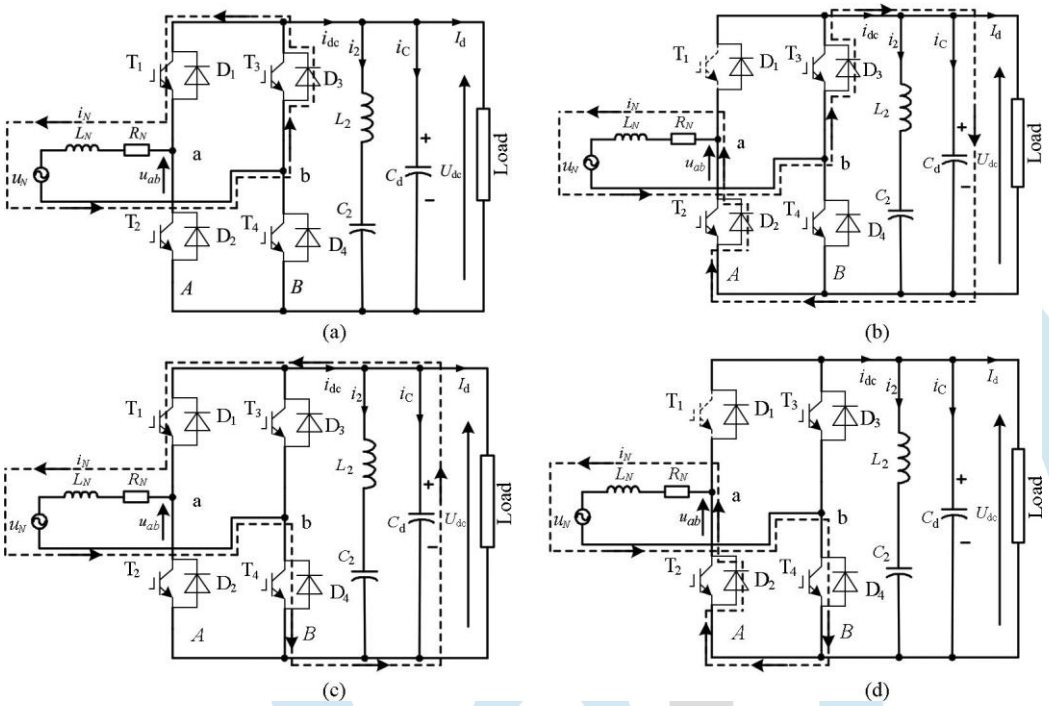

Fig. 3. Single-phase PWM rectifier circuit topology: (a) normal topology in command (1010) and (1000), (b) faulty topology in command (1010) and (1000), (c) normal topology in command (1001), (d) faulty topology in command (1001), and the dash trace is the flowing direction of the catenary current.

A. IGBT Open-Circuit Fault Analysis

In order to clearly analyse the IGBT open-switch fault conditions in the single-phase PWM rectifier, it is assumed that the upper switch of leg A is an open-circuit faulty switch, T_1. It is assumed that the catenary current's reference direction is from the traction winding to the rectifier. As shown in Fig. 2, the current could flow through the bypass diode D_1 associated with the faulty switch when the catenary current is positive. Thus, there is no change in the catenary current waveform during the first half current cycle after the open-switch fault occurs. However, when the catenary current is negative, current cannot flow through the bypass diode D_1. If the catenary current is negative, the rectifier cannot operate normally when the command signals are (1010), (1001), and (1000).

Beginning with the command signal (1010), the upper switch of leg A is turned on when the switch T_1 is in the normal condition. The catenary current flows through the bypass diode, D_3, and switch, T_1, shown as Fig. 3(a). In this context, the grid voltage charges the inductor to facilitate energy storage, and the amplitude of the catenary current is increasing. Meanwhile, the energy stored in the dc-link capacitor is released to the load. Thus, the dc-link voltage is reducing.

However, if switch T_1 in leg A is open circuited due to a fault condition while its firing signal is high, the energy stored in the inductor is released. Since the current flowing through an inductor cannot change instantaneously, it must flow through the bypass diode D_2 and D_3, shown as Fig. 3(b). In this condition, the grid voltage and the inductor charge the dc-link capacitor simultaneously. Thus, the amplitude of the catenary current is declining and the dc-link voltage is increasing. But, due to the reducing of the catenary current amplitude, the increasing amplitude of dc-link voltage is limited, and depends on the load. When the command is (1001), switch T_1 in leg A and switch T_4 inlegBareturnedonwhenT_1 not faulted, shown as Fig.3(c). In this case, both

the grid voltage and the dc-link voltage charge the inductor, resulting in energy storage. Therefore, the amplitude of the catenary current increases sharply, and the dc-link voltage is reducing. But due to the open-circuit fault of switch T_1, the catenary current can only flow through the bypass diode D_2 and switch T_4, shown as Fig. 3(d). In this case, only the grid voltage charges the inductor. Thus, the increasing amplitude of catenary current is less than those in normal mode. Also, the energy stored in the dc-link capacitor is released to the load. So, the dc-link voltage is reducing. With the command (1000), both the fault and the normal mode are the same as command (1010). Since the signal (1000) is effective only when the switch operates during the dead-time, this command signal has little effect on the rectifier when there is an open-circuit fault in T_1.Therefore, the amplitudes of the catenary current and the dc link voltage both are declining due to an open-circuit fault in T_1, shown as Fig. 4. All the previous explanations can be extended to the remaining switches, T_2, T_3, and T_4.

B. Diode Open-Circuit Fault Analysis

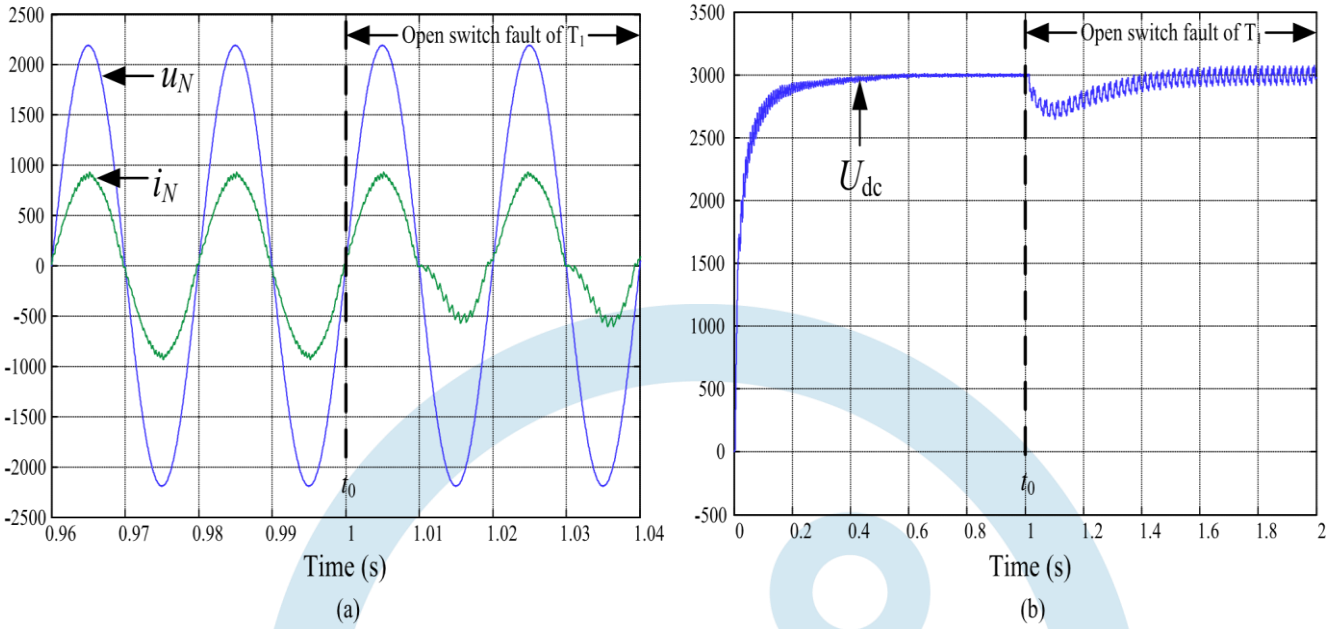

Fig. 4. Simulation results when the switch T_1 occurs open-circuit fault (t =1 s): (a) grid voltage and current waveforms (u_N/V, i_N /A), (b) DC-link voltage waveform (U_{dc}/V).

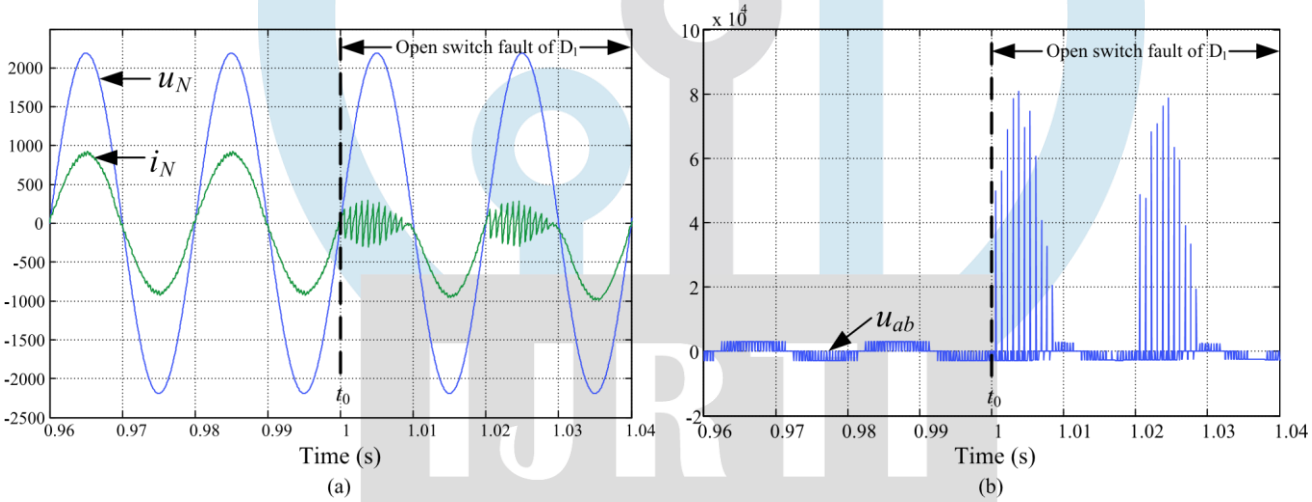

Fig. 5.Simulation results when the diode D_1 occurs open-circuit fault (t = 1s): (a) grid voltage and current waveforms (u_N/V, i_N /A), (b) input voltage of the rectifier (u_{ab}/V)

As for diode open-circuit fault, it is also assumed that the upper diode of leg A is an open-circuit faulty diode, D_1. As shown in Fig. 2, the catenary current flows through the switch,T_1, or the clamping diode, D_2, when the current is negative. The clamping diode D_1 does not work during this half period of catenary current. Thus, there is no change in the catenary current waveform when the current is negative after the diode D_1 occurring open-circuit fault. However, when the catenary current is positive, current has no way to flow through unless the switch T_2 is turned on, shown as Fig. 5(a). Since the current flowing through an inductor cannot change instantaneously, this abrupt mutation may result in a sharp increase of the inductor voltage. According to the Kirchhoff's law, the input voltage of the rectifier rises abruptly, which may lead to a tremendous voltage stress on the switches of leg A, T_1 and T_2. As shown in the Fig. 5(b), the input voltage could be 50 000 V in the brief moment when the catenary current is open. The rated blocking voltage of the IGBT is 6.5 kV. Therefore, the abnormal voltage stress caused by the diode open-circuit fault is much higher than the blocking voltage of the IGBT, which may result in the IGBTs overvoltage failure in a short time. [32] and [33] mentioned that the reason of the IGBT overvoltage breakdown failure is due to the thermal stresses and heat accumulations in the junction, which may result in an IGBT short circuit during a short transient. Thus, diode open-circuit fault is one of the most damaging failures in the traction converter. Moreover, hardware based protection schemes are employed in control circuits of the IGBTs to prevent the abnormal overcurrent and overvoltage issues. Therefore, this paper focuses on the open-switch fault diagnosis method for IGBTs of the single-phase PWM rectifier.

III. MLD MODEL OF A SINGLE-PHASE PWM RECTIFIER

The MLD model proposed previously provides a framework for modeling and controlling systems described by interdependent physical laws, logical rules, and operating constraints [34]. It is often used in optimal control, predictive control and fault diagnosis applications.

As shown in Fig. 2, the continuous state space model of the single-phase PWM rectifier is described as

$$u_N = L_N \frac{di_N}{dt} + R_N i_N + u_{ab}. \quad (2)$$

An auxiliary binary variable δ is defined as follows to illustrate the changing of the catenary current:

$$[\delta = 1] \leftrightarrow [i_N > 0]$$

$$[\delta = 0] \leftrightarrow [i_N < 0]. \quad (3)$$

From the truth table, the function of the ideal binary switch is described

$$\begin{cases} S_A = \bar{s}_2(s_1 + \delta) \\ S_B = \bar{s}_4(s_3 + \bar{\delta}) \end{cases} \quad (4)$$

As shown in Fig. 2, the input voltage of rectifier, u_{ab}, is expressed as

$$u_{ab} = (S_A - S_B)U_{dc}. \quad (5)$$

Substituting (5) into (2) obtains the MLD model of single phase PWM rectifier as

$$\frac{di_N}{dt} = \frac{u_N}{L_N} - \frac{R_N i_N}{L_N} - \frac{U_{dc}}{L_N}\left[\bar{s}_2(s_1 + \delta) - \bar{s}_4(s_3 + \bar{\delta})\right]. \quad (6)$$

Then, an auxiliary binary variable γ is defined as follows:

$$\gamma = \bar{s}_2(s_1 + \delta) - \bar{s}_4(s_3 + \bar{\delta}). \quad (7)$$

Therefore, (6) can be rewritten as

$$\dot{i}_N = Ai_N + B_1 u_N + B_2 \gamma \quad (8)$$

where coefficients A, B_1, and B_2 are defined as: $A = -R_N/L_N$, $B_1 = 1/L_N$, and $B_2 = -U_{dc}/L_N$. As shown in (8), the continuous state variable, i_N, is dependent on the discrete variable, γ. Furthermore, γ is dependent on the command signals of the IGBTs and the polarity of continuous state variable, δ. Thus, the single-phase PWM rectifier is a hybrid system affected jointly by continuous variables and discrete variables.

IV. OPEN-SWITCH FAULT DIAGNOSTIC METHOD

In reality, some or even all variables of the single-phase PWM rectifier may be different from those of the normal condition when there is an open-circuit fault in the switches. The basic idea of the open-switch fault diagnosis method based on MLD model is via analysing and evaluating the system residual, which is obtained by continuously comparing the actual system output with the one of the MLD model. The residual is zero or within a small threshold when the system is normally operating. On the contrary, the amplitude of the system residual will increase sharply during a fault.

A. Residual Generation

According to (8), the state estimator of single-phase PWM rectifier can be described as

$$\hat{\dot{i}}_N = A\hat{i}_N + B_1 u_N + B_2 \gamma. \quad (9)$$

As discussed above, the topology of the system is determined by the discrete variable, γ. In the normal case, the discrete input variable of the actual system is the same as that of the state estimator. Therefore, the output of the state estimator is close to that of the actual system when the MLD model is designed precisely. However, in the case of an open-circuit fault, the discrete input variable of the actual system is changed to $\gamma'(\gamma' \neq \gamma)$, where as the discrete input variable of state estimator is still γ. Thus, the outputs of these two systems are different. Therefore, the system residual can be defined as

$$\tilde{i}_N = i_N - \hat{i}_N. \quad (10)$$

From (8) and (9), one obtains (11).

$$\dot{\tilde{i}}_N = A\tilde{i}_N + B_2(\gamma' - \gamma). \quad (11)$$

Assuming an open-circuit fault in T_1 under the full bridge rectifier operation, the command signal is always inactive for T_1, namely, $s_1' \equiv 0$. Then, the discrete input variable of the rectifier is changed as

$$\gamma' = \bar{s}_2\delta - \bar{s}_4(s_3 + \bar{\delta}) \quad (12)$$

Therefore, the system residual can be rewritten as

$$\dot{\tilde{i}}_N = A\tilde{i}_N + B_2(-s_1\bar{s}_2). \quad (13)$$

Assuming that the initial value of the system residual is zero, the residual can be obtained by solving equation (13), as

$$\tilde{i}_{NT_1} = \frac{s_1\bar{s}_2U_{\mathrm{dc}}}{R_N}\left(1 - e^{-\frac{R_N}{L_N}t}\right) \quad (14)$$

From (14), one can see that the system residual is always positive and dependent on the dc-link voltage, and the traction winding leakage inductance and resistance when T_1 is faulted.

$$\tilde{i}_{NT_2} = -\frac{s_2(s_1 + \delta)U_{\mathrm{dc}}}{R_N}\left(1 - e^{-\frac{R_N}{L_N}t}\right) \quad (15)$$

$$\tilde{i}_{NT_3} = -\frac{s_3\bar{s}_4U_{\mathrm{dc}}}{R_N}\left(1 - e^{-\frac{R_N}{L_N}t}\right) \quad (16)$$

$$\tilde{i}_{NT_4} = \frac{s_4\left(s_3 + \bar{\delta}\right)U_{\mathrm{dc}}}{R_N}\left(1 - e^{-\frac{R_N}{L_N}t}\right) \quad (17)$$

All the aforementioned analysis about switch T_1 can be extended to the remaining switches. Thus, the system residual when T_2, T_3, or T_4 is in the open-circuit fault is shown as follows, respectively.

B. Fault Detection Threshold

From (14) to (17), it is clear that the system residual has a maximum, shown as

$$|t_N T_n|_{max=\frac{U_{dc}}{R_N}} \quad (18)$$

where n = 1, 2, 3, 4. The maximum value depends only on the dc-link voltage and the traction winding resistance. In an actual system, the values of dc-link voltage and traction winding resistance are, say, 2700–3600 V and 0.068 Ω, respectively. Then the maximum of the system residual is quite large, reaching 53 000, which makes detection easy.

TABLE II
OPEN-CIRCUIT FAULT DIAGNOSIS SIGNATURES

Faulty switch	Residual	
	Before (1010)	After (1010)
T_1	0	No Change
T_2	>0 / <0 / <0 / >0	$= 0$
T_3	0	No Change
T_4		$= 0$

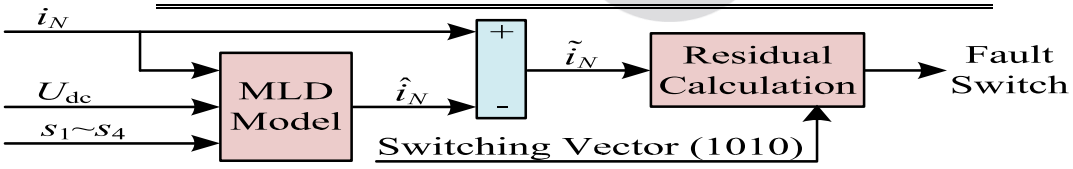

Fig. 6.Block diagram of the diagnosis method based on MLD model.

n the actual traction converter system, the estimation error of the MLD model obviously exists due to estimation errors in the parameters (e.g., U_{dc}) and the measurement noise. Consequently, the definition of the fault detection threshold value d is given as 500 according to a trade off between the detection speed and the robustness against the false alarms.

However, from (14) to (17), the system residual is positive when switch T_1 or switch T_4 experiences an open-circuit fault. On the contrary, the system residual is negative when switch T_2 or switch T_3 experiences an open-circuit fault. The faulty switch cannot be identified specifically.

C. Faulty IGBT Identification

In order to located the faulty IGBT among the two potential candidates, the switching vector of the rectifier is changed to (1010) after the fault detection. As a result, the system residual is zero when switch T_2 or T_4 has an open-circuit fault, but there is no change in the residual when switch T_1 or T_3 are faulty. Thus, the open-switch fault diagnosis for the single-phase PWM rectifier can be achieved by calculating and monitoring the only residual, which results from a continuous comparison of the MLD-based model output with that of the actual system. The fault diagnostic signatures presented in Table II can be used to locate the faulty switch. Thus, the block diagram of the open-switch diagnosis method based on the MLD model can be summarized as Fig. 6.

D. Fault Diagnosis Time

The fault diagnosis time includes two parts, fault detection time and fault identification time, respectively, shown as

$$tF\,DI = tF\,D + tF\,I \qquad (19)$$

where $t_{F\,DI}$ is the fault diagnosis time, $t_{F\,D}$ is the fault detection time, and $t_{F\,I}$ is the fault identification time. It is clear that the fault detection time $t_{F\,D}$ is dependent on the fault detection threshold value d. From (14), the minimum of the fault detection

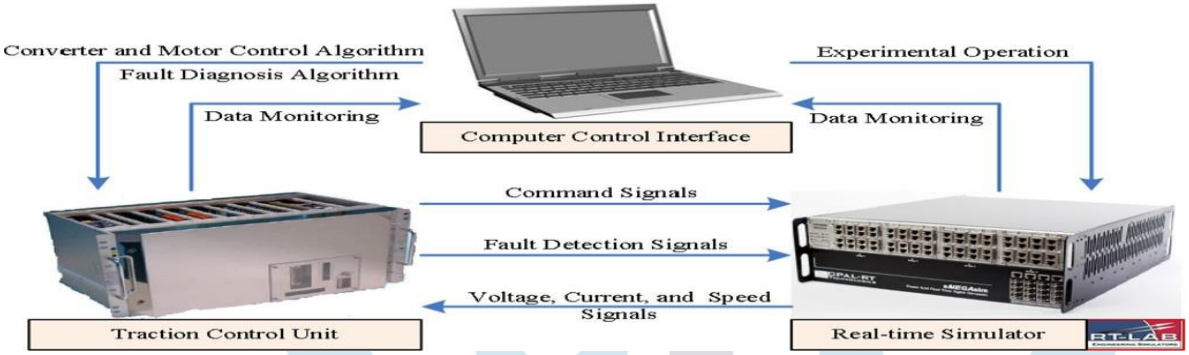

Fig. 7.Diagram of the experimental setup.

time $t_{F\,D}$ can be shown as (20).

$$t_{FD} = -\frac{L_N}{R_N}\ln\left(1 - d\cdot\frac{R_N}{U_{\mathrm{dc}}}\right). \qquad (20)$$

Moreover, the fault identification time $t_{F\,I}$ is mainly dependent on the control frequency of the core control chip, and only dozens of microseconds. Thus, the fault diagnosis time is mainly decided by the fault detection time. When the fault detection threshold value d is given as 500, the minimum of fault detection time $t_{F\,D}$ is about 400 μs, which is good enough for IGBT open-switch fault diagnosis. However, the increasing speed of the system residual amplitude is also dependent on the command signals of the rectifier when an open-switch fault is in T_1, according to (14). Thus, the fault diagnosis time in practice would be several times larger than the theoretic minimum diagnosis time.

V. EXPERIMENTAL RESULTS

In order to verify the effectiveness and accuracy of the proposed fault diagnosis method in the electrical railway traction system, shown as Fig. 2, the three-phase PWM inverter-fed induction motor is applied as the load of the single-phase PWM rectifier. The experimental platform comprises a TCU as a controller, whose core control chip is TMS320F2812, an RT-LAB simulator DS5600, and a computer as a real-time control interface, as shown in Fig. 7. The hardware circuit, including the open-switch fault model of the rectifier, three-phase PWM inverter, induction motor, and the sensors are realized in the RTLAB simulator. The open-switch fault is introduced by removing the IGBT. The TCU receives the voltage, current, and speed signals from the RT-LAB simulator and sends the IGBT command and fault detection signals after the A/D conversion and calculations. Together with the Matlab/Simulink and RT-LAB control interface, the controller provides a real-time control, monitoring of the overall system at a sampling time of 40 μs. The parameters of the converter and induction motor are given in Tables III and IV, respectively.
In order to ensure a unity power factor operation and dc link voltage regulation, a proportional integrator (PI) controller in the external control loop and a proportional resonant (PR) controller in the inner loop control are adopted in the rectifier-

TABLE III
PARAMETERS OF CONVERTER

Parameter	Symbol	Value
RMS grid voltage	*uN*	1550 V
Traction winding leakage inductor	L_N	2.3 mH
Traction winding resistor	R_N	0.068 Ω
Dc-link voltage	*U*dc	2700–3600 V
Dc-link capacitor	C_d	3 mF
Series resonant circuit inductor	L_2	0.603 mH
Series resonant circuit capacitor	C_2	4.56 mF
Rectifier switching frequency	*fR*	350 Hz
Highest inverter switching frequency	f_I	500 Hz

TABLE IV
PARAMETERS OF INDUCTION MOTOR

Parameter	Symbol	Value
Stator resistance	R_s	0.1065 Ω
Stator leakage inductance	*Lls*	1.31 mH
Rotor resistance	R_r	0.0663 Ω
Rotor leakage inductance	*Llr*	1.93 mH
Mutual inductance	*Lm*	53.6 mH
Rated voltage	*U*rate	2700 kV
Rated speed	*n*rate	4100 (r/min)
Rated frequency	*f*srate	138 Hz
Rated output power	*P*rate	562 kW
Rated slip frequency	*s*rate	0.04
Number of the pole pairs	n_p	2

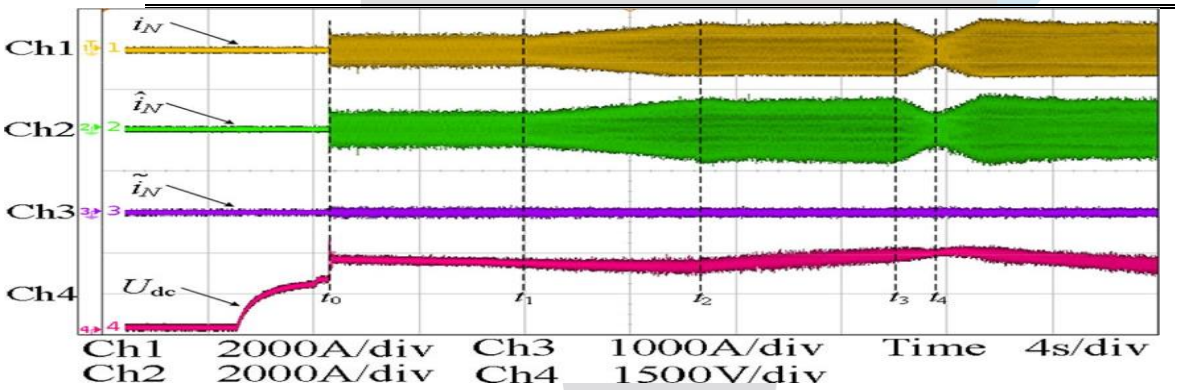

Fig.8. Experimentally measured results in the normal condition (i_N/A, $\hat{i}_N$/A, $\tilde{i}_N$/A, u_{dc}/V).

side control. Space vector pulse width modulation and indirect field-oriented control are applied in the inverter-side control to achieve good dynamic responses of motor speed.

he experimentally measured result when the traction drive system is operating in normal operation condition is shown as Fig. 8, where the Ch1 trace is the actual signal of the catenary current from the current sensor; the Ch2 trace is the estimated signal from the MLD-based model; the Ch3 trace is the system residual; and the Ch4 trace is the dc-link voltage signal. As shown in Fig. 8, the rectifier and inverter are started at the moment of t_0 and t_1, respectively. The induction motor is in constant-torque operation between t_1 and t_2, and in constant power operation after t_2. Then, the dc-link voltage increases from 2700 to 3600 V. Finally, the induction motor begins to brake at t_3. Thus, the traction drive system is working as regenerative braking mode after t_4. It is clear that the catenary current and the estimated results of the MLD-based model are almost coinciding, and there is no misdiagnosis, regardless the operation of the induction motor and the fluctuation of the dc-link voltage, even if the rectifier is working as a dc–ac converter. The experimentally measured results when the rectifier is in open-switch fault are shownas Fig. 9.

In Fig. 9, the Ch4 trace is the fault detection output signal. When the rectifier is in the normal condition, the MLD-based

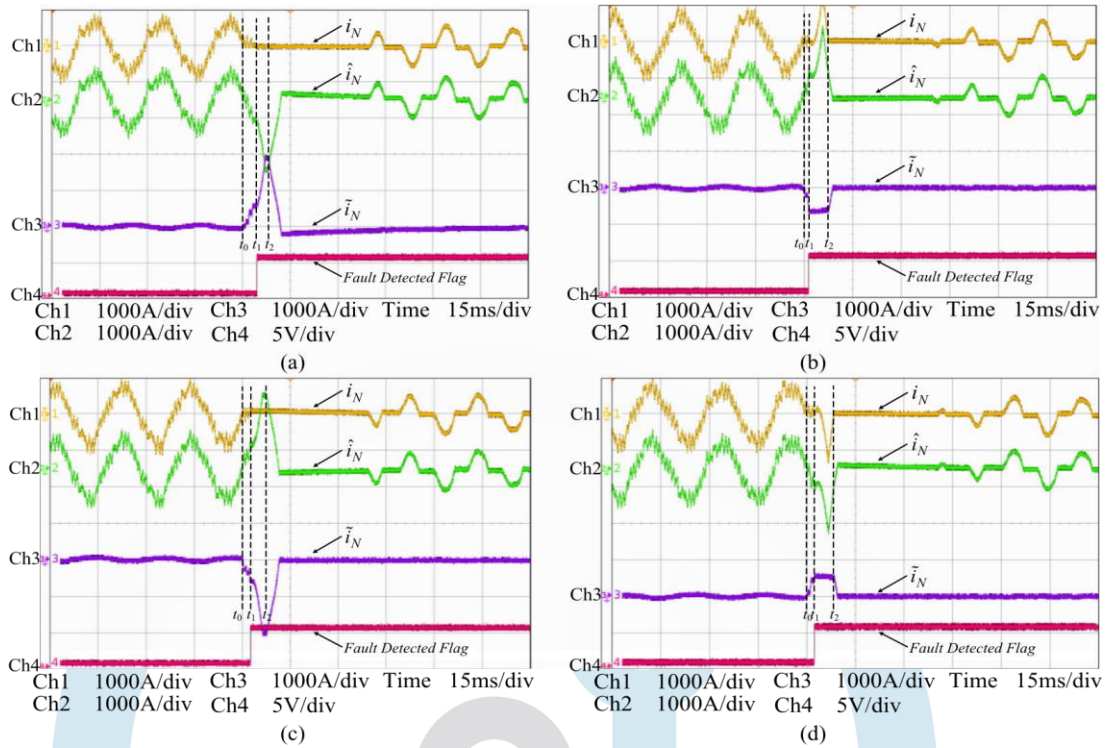

model output is nearly the same as the output of the current sensor. The system residual is therefore nearly zero and far from the fault detection threshold value, *d*. Since the inverter fed induction motor is an inductive load, the catenary current contains not only inherent low-order odd harmonics resulted from the circuit topology and the control algorithm, but also high-order harmonics caused by power switches. As shown in the figures, the open-switch fault is introduced at t_0, leading to a distortion in the catenary current signal. Nevertheless, the estimating signal of the MLD-based model is unchanged due to the normal command signals. Therefore, the amplitude of the system residual is increasing drastically, as shown in Fig. 9. Moreover, the residual is positive when an open-switch fault is in switch T_1 or T_4, and it is negative when an open-switch fault is in T_2 or T_3, as presented in Fig. 9(a), (d) and (b), (c), respectively. When the amplitude of the system residual exceeds the fault detection threshold value, *d* at t_1, the command signals are changed to (1010). In Fig. 9(d), it is shown that the system residual decreases immediately whereas it keeps increasing in Fig. 9(a). Thus, *it can make a distinction between switch T_1 and T_4*. It is also clear from Fig. 9 that the fault diagnosis time is less than 3 ms. In order to monitor the system residual, the turn-off signals of IGBTs are delayed to t_2, and then the rectifier works as a full diode bridge. Thus, the open-switch fault detection and the isolation of the single-phase PWM rectifier are successfully accomplished.

In order to examine the reliability of the proposed method when the grid voltage is fluctuating, some experimental tests are accomplished, shown as Fig. 10. The RMS grid voltage is increased from 1550 to 1800 V and with some high-order harmonics. Due to these changes in grid voltage, the catenary current also has more high-order harmonics, compared with Fig. 9. But the proposed method can also detect the faulty switch accurately with no misdiagnosis.

Moreover, the single-phase PWM rectifier is an ac–dc converter when the induction motor works as a traction motor, while a dc–ac converter when the induction motor works as a generator. In order to validate the proposed method when the rectifier operates as an inverter, experimental results are considered when the traction drive system works as regenerative braking mode, shown as Fig. 11. Since the load is different in Fig. 9, as compared to Figs. 8 and 11, it can also be seen that the proposed fault diagnosis method is not sensitive to the load, even when the load is light.

Fig. 9. Experimentally measured results for (a) T_1 open-switch fault detection, (b) T_2 open-switch fault detection, (c) T_3 open-switch fault detection, (d) T_4 open-switch fault detection (i_N/A,$\hat{i}_N$/A,$\tilde{i}_N$/A, *F*/V).

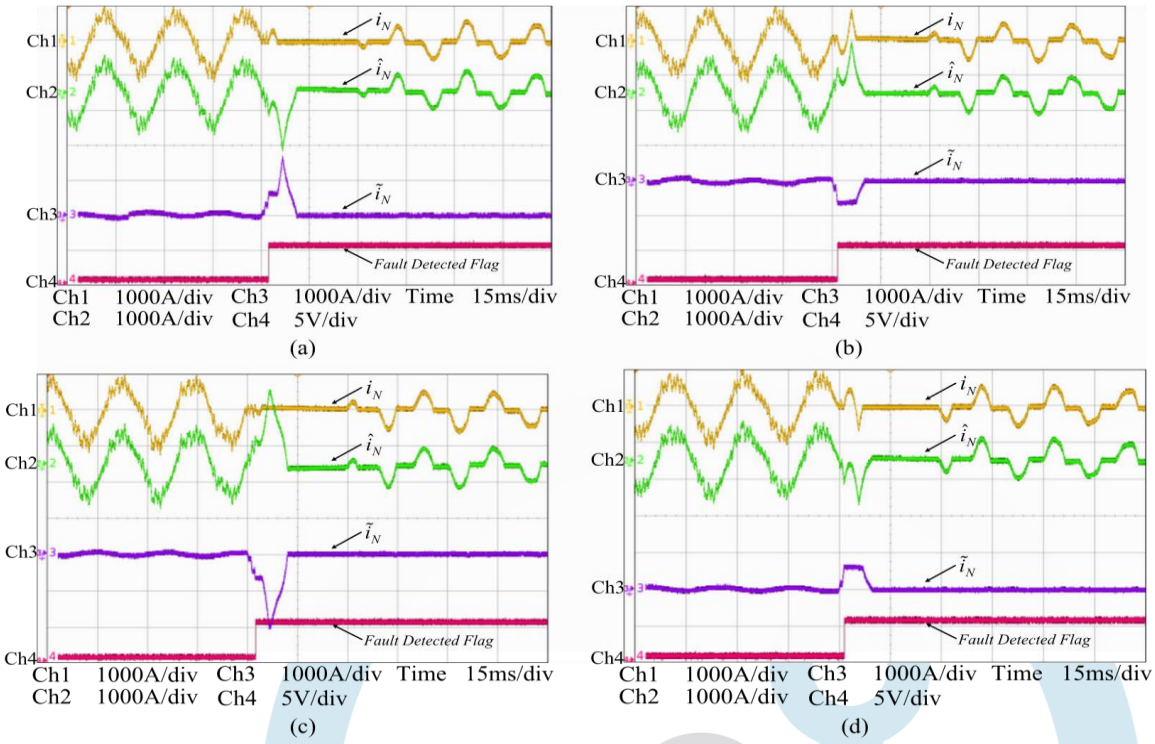

Fig. 10. Experimentally measured results for (a) T_1 open-switch fault detection, (b) T_2 open-switch fault detection, (c) T_3 open-switch fault detection, (d) T_4 open-switch fault detection under the condition of the grid voltage variation (i_N/A,$\hat{}i_N$/A,$\tilde{}i_N$/A, F/V).

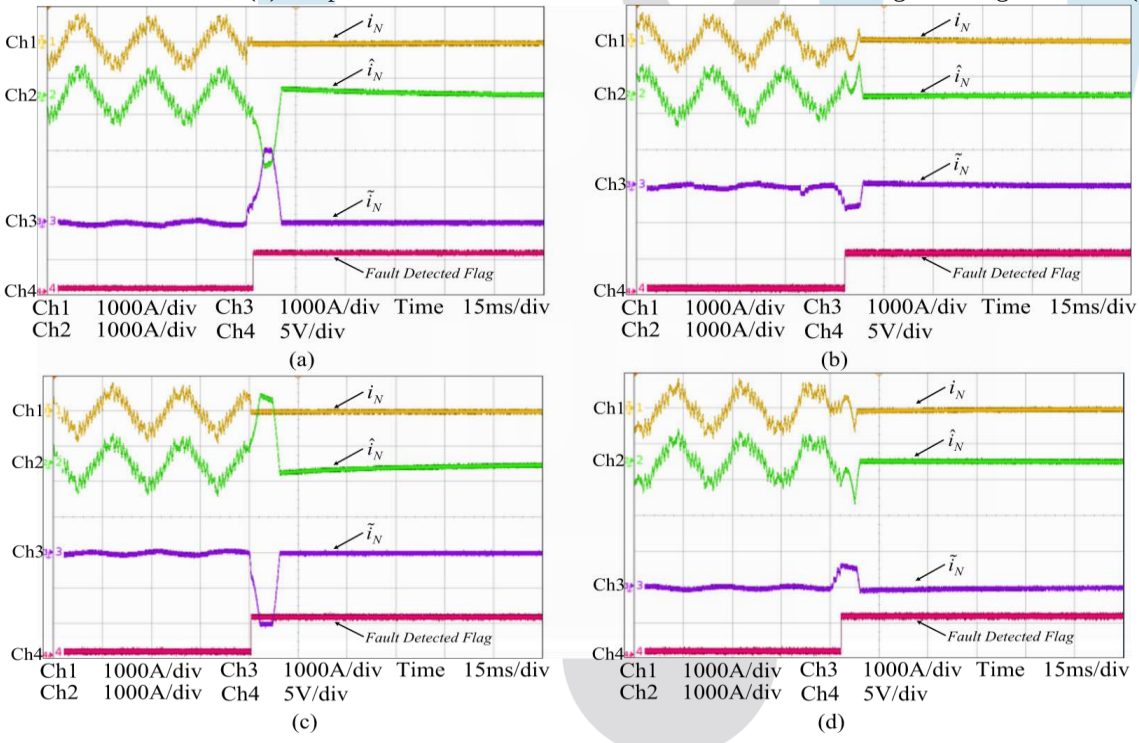

Fig. 11. Experimentally measured results for (a) T_1 open-switch fault detection, (b) T_2 open-switch fault detection, (c) T_3 open-switch fault detection, (d) T_4 open-switch fault detection in the regenerative braking mode (i_N/A,$\hat{}i_N$/A,$\tilde{}i_N$/A, F/V).

From the dynamic process, as shown in Figs. 10 and 11, it could be concluded that the proposed diagnosis method is not sensitive to the grid voltage and the load since the system residual is only related to the dc-link voltage and the traction winding resistance according to (18).Therefore, it is quite suitable for use in the railway traction applications owing to the high reliability and the low cost.

VI. CONCLUSION

A new and simple approach to diagnose open-switch fault in single-phase PWM rectifier using an MLD-based model approach has been proposed in this paper. The difference between MLD-based model of the single-phase PWM rectifier and the actual operation is used to detect which switch is faulted. This model-based method requires no additional hardware. Only the switch command signals, the measured catenary current and the dc-link voltage, which are already available in high-speed trains

and industrial drives, are used. As a result, this method is independent to the grid voltage and the system load. But this method takes effect only when the faulty IGBT is gated. It is not effective when the rectifier works as a full diode bridge due to the dependence to the command signals of the rectifier. The system residual results from a continuous comparison of the MLD-based model output with that of the actual system, which takes into account the dead times of the switch operation during the setting up of the MLD-based model.

This diagnosis method is quite reliable, capable of fast diagnosis at a low computational requirement with only one threshold value needed to locate the faulty switch of the rectifier. Its detection time is shorter than 3 ms, which implies a secondary fault in other components can be avoided, which is very suitable for improving the reliability and efficiency of the fault maintenance of the traction converters. Moreover, the experimental evaluation of the proposed method confirms that it is especially suitable for integration into the controller of the variable-speed drives with a high dynamic performance.

REFERENCES

[1] R. Hill, "Electric railway traction—Part II. Traction drives with three phase induction motors," *Power Eng. J.*, vol. 8, no. 3, pp. 143–152, Jun. 1994.

[2] A. Steimel, "Electrical railway traction in Europe," *IEEE Ind. Appl. Mag.*, vol. 2, no. 6, pp. 6–17, Nov./Dec. 1996.

[3] A. D. Cheok, S. Kawamoto, T. Matsumoto, and H. Obi, "High power AC/DC converter and DC/AC inverter for high speed train applications," in *Proc. IEEE TENCON*, Sep. 2000, pp. 423–428.

[4] S. Yang, D. Xiang, A. Bryant, P. Mawby, L. Ran, and P. Tavner, "Condition monitoring for device reliability in power electronic converters: A review,"*IEEETrans.PowerElectron.*,vol.25,no.11,pp.2734–2752,Nov. 2010.

[5] B. Ji, V. Pickert, W. Cao, and B. Zahawi, "*In situ* diagnostics and prognostics of wire bonding faults in IGBT modules for electric vehicle drives," *IEEE Trans. Power Electron.*, vol. 28, no. 12, pp. 5568–5577, Dec. 2013.

[6] B. Ji, X. Song, W. Cao, V. Pickert, Y. Hu, J. W. Mackersie, and G. Pierce, "*In situ* diagnostics and prognostics of solder fatigue in IGBT modules for electric vehicle drives," *IEEE Trans. Power Electron.*, vol. 30, no. 3, pp. 1535–1543, Mar. 2015.

[7] F. Abrahamsen, F. Blaabjerg, K. Ries, and H. Rasmussen, "Fuse protection of IGBT's against rupture," in *Proc. IEEE Nordic Workshop Power Ind. Electron.*, Jun. 2000, pp. 64–68.

[8] I.Jlassi,J.O.Estima,S.K.ElKhil,N.M.Bellaaj,andA.J.Cardoso,"Multiple open-circuit faults diagnosis in back-to-back converters of PMSG drives for wind turbine systems," *IEEE Trans. Power Electron.*, vol. 30, no. 5, pp. 2689–2702, May 2015.

[9] R. Ribeiro, C. Jacobina, E. Da Silva, and A. Lima, "Fault detection of open-switch damage in voltage-fed PWM motor drive systems," *IEEE Trans. Power Electron.*, vol. 18, no. 2, pp. 587–593, Mar. 2003.

[10] D. R. Espinoza-Trejo, D. U. Campos-Delgado, G. Bossio, E. Barcenas, J. E. Hernandez-Diez, and L. F. Lugo-Cordero, "Fault diagnosis scheme for open-circuit faults in field-oriented control induction motor drives," *IET Power Electron.*, vol. 6, no. 5, pp. 869–877, May 2013.

[11] S. Shao, P. W. Wheeler, J. C. Clare, and A. J. Watson, "Fault detection for modular multilevel converters based on sliding mode observer," *IEEE Trans. Power Electron.*, vol. 28, no. 11, pp. 4867–4872, Nov. 2013.

[12] D. U. Campos-Delgado and D. R. Espinoza-Trejo, "An observer-based diagnosis scheme for single and simultaneous open-switch faults in induction motor drives," *IEEE Trans. Ind. Electron.*, vol. 58, no. 2, pp. 671–679, Feb. 2011.

[13] Q. T. An, L. Z. Sun, K. Zhao, and L. Sun, "Current residual vector-based open-switch fault diagnosis of inverters in PMSM drive systems," *IEEE Trans. Power Electron.*, vol. 30, no. 5, pp. 2814–2827, May 2015.

[14] S. M. Jung, J. S. Park, H. W. Kim, K. Y. Cho, and M. J. Youn, "An MRAS based diagnosis of open-circuit fault in PWM voltage source inverters for PM synchronous motor drive systems," *IEEE Trans. Power Electron.*, vol. 28, no. 5, pp. 2514–2526, May 2013.

[15] J. Zhang, J. Zhao, D. Zhou, and C. Huang, "High-performance fault diagnosis in PWM voltage-source inverters for vector-controlled induction motor drives," *IEEE Trans. Power Electron.*, vol. 29, no. 11, pp. 6087–6099, Nov. 2014.

[16] W. Sleszynski, J. Nieznanski, and A. Cichowski, "Open-transistor fault diagnostics in voltage-source inverters by analyzing the load currents," *IEEE Trans. Ind. Electron.*, vol. 56, no. 11, pp. 4681–4688, Nov. 2009.

[17] Q. T. An, L. Z. Sun, K. Zhao, and L. Sun, "Switching function model based fast-diagnostic method of open-switch faults in inverters without sensors," *IEEE Trans. Power Electron.*, vol. 26, no. 1, pp. 119–126, Jan. 2011.

[18] C.ChoiandW.Lee, Design and evaluation of voltage measurement-based sectoral diagnosis method for inverter open switch faults of permanent magnet synchronous motor drives," *IET Elect. Power Appl.*, vol. 6, no. 8, pp. 526–532, Sep. 2012.

[19] N. M. A. Freire, J. O. Estima, and A. J. M. Cardoso, "A voltage-based approachwithoutextrahardwareforopen-circuitfaultdiagnosisinclosedloop PWM AC regenerative drives," *IEEE Trans. Ind. Electron.*, vol. 61, no. 9, pp. 4960–4970, Sep. 2014.

[20] M.AwadallahandM.Morcos,"Automaticdiagnosisandlocationofopenswitch fault in brushless dc motor drives using wavelets and neuro-fuzzy systems," *IEEE Trans. Energy Convers.*, vol. 21, no. 1, pp. 104–111, Mar. 2006.

[21] S. Khomfoi and L. M. Tolbert, "Fault diagnosis and reconfiguration for multilevel inverter drive using AI-based techniques," *IEEE Trans. Ind. Electron.*, vol. 54, no. 6, pp. 2954–2968, Dec. 2007.

Vinay kumar K was born in Relakunta, Telangana in 1989 and he completed his B.Tech in Electrical and Electronics Engineering from BITS, Narsampet in the year2011and the M.Tech degree from CVSR, Hyderabad in 2015.Presently,he is working as an Assistant Professor in Bhoj Reddy Engineering College for Women, Hyd. His areas of interest Include Power Systems, and Power Electronics.

SK.VALI was born in B.Gangaram, Telangana in 1989 and he completed his B.Tech in Electrical and Electronics Engineering from SSIT, B.Gangaram in the year 2010 and the M.Tech degree from Jawaharlal Nehru Technological University, Kakinada in 2012. Presently, he is working as an Assistant Professor in Bhoj Reddy Engineering College for Women, Hyd. His areas of interest Include Power Electronics, Electrical Machines and drives.

Ravikumar K was born in Hyderabad, Telangana in 1983 and she completed her B.Tech in Electrical and Electronics Engineering from MVSR, Hyderabad in the year 2005 and the M.Tech degree from VIST, Nalgonda in 2015. Presently, he is working as an Assistant Professor in Bhoj Reddy Engineering College for Women, Hyd. his areas of interest include Power Systems, and Power Electronics.